17. *Geomagnetic Anomaly on Volcanoes with Relation to Their Subterranean Structure.*

By Izumi YOKOYAMA,

Earthquake Research Institute.

(Read November 27, 1956.—Received March 31, 1957.)

Summary

Dip-survey on the volcanic islands of the Seven Izu Islands at the south of Japan Proper has been almost completed. These volcanic islands differ in dimension and geological structure and therefore exhibit various features of distribution of geomagnetic anomaly. The writer, in this paper, tries to interpret the anomaly in relation to the subterranean structure of the volcanoes. To attain the object, the following items are considered:

1. Representation of geomagnetic anomaly on a volcano by a dipole-field.
2. Magnetization of igneous rocks and its range.
3. Bulk-density of the mountain-mass.
4. Determination of depth of sources by analysing the vertical component in the geomagnetic field on Volcano Mihara.
5. Some knowledge obtained by a gravity survey on Volcano Mihara.
6. Some discussions on parasitic cones of Volcano Mihara.
7. Geomagnetic anomaly around the craters of volcanoes.
8. Some information obtained by aeromagnetic surveys over the volcanoes in Alaska.

Introduction

Many geophysicists have observed the geomagnetic field on volcanoes and recently even aeromagnetic surveys are carried out over volcanoes in U.S.A. It would be an endless task to cite the examples of dip-survey especially in Japan. One of the problems for a volcanologist, the writer thinks, is how to utilize significantly the analyses of the geomagnetic anomaly together with other methods in order to obtain some knowledge in relation to the subterranean structure of the volcanoes even if there is a limit to it. Here, the writer discuss this problem with reference to the geomagnetic anomalies on the Seven Izu Islands.

The Seven Izu Islands are composed of a number (more than seven) of volcanic islands including active, dormant and extinct Quaternary

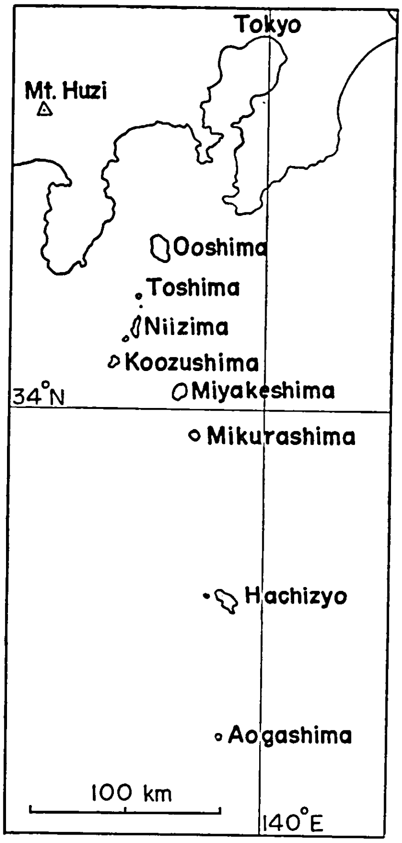

Fig. 1. The Seven Izu Islands.

volcanoes while their rocks are discriminated into basalt, andesite and liparite. This archipelago runs southward perpendicularly to Japan Proper and continues to Mariana Islands via Ogasawara (Bonin) Islands and Iwoo (Sulphur) Islands.

T. Minakami[1] carried out a dip-survey on Miyakeshima Island in 1940 and R. Takahasi and T. Nagata[2] observed the geomagnetic anomaly on Ooshima Island in 1936. T. Rikitake and the writer[3] have been increasing the observation of dip-angle and other components of geomagnetic field on Ooshima Island since 1950. The writer has almost completed dip-surveys on the other islands of the Seven Izu Islands. These results are shown in Fig. 2 and Table I. Fig. 3 shows the mean topographic profiles of each islands obtained by averaging in eight directions.

1. Representation of geomagnetic anomaly on a volcano by a dipole-field

Regarding interpretation of geomagnetic anomalies on volcanoes, there have been several opinions: Anomalous geomagnetic field was represented by uniform magnetization of the mountain-mass which was assumed to be of ellipsoidal or circular conical shape. The former approximation is called the Haalck-Koenigsberger's method and T. Minakami[4,5,6] adopted it with the intention of interpreting the geomagnetic

1) T. MINAKAMI, *Bull. Earthq. Res. Inst.*, **19** (1940), 356.
2) R. TAKAHASI and T. NAGATA, *Bull. Earthq. Res. Inst.*, **15** (1937), 441.
3) T. RIKITAKE, *Bull. Earthq. Res. Inst.*, **29** (1951), 161.
T. RIKITAKE, I. YOKOYAMA, A. OKADA and Y. HISHIYAMA, *Bull. Earthq. Res. Inst.*, **29** (1951), 583.
4) T. MINAKAMI, *Bull. Earthq. Res. Inst.*, **18** (1940), 178.
5) H. TSUYA and T. MINAKAMI, *Bull. Earthq. Res. Inst.*, **18** (1940), 338.
6) T. MINAKAMI and S. SAKUMA, *Bull. Volcanologique*, **18** (1956), 77.

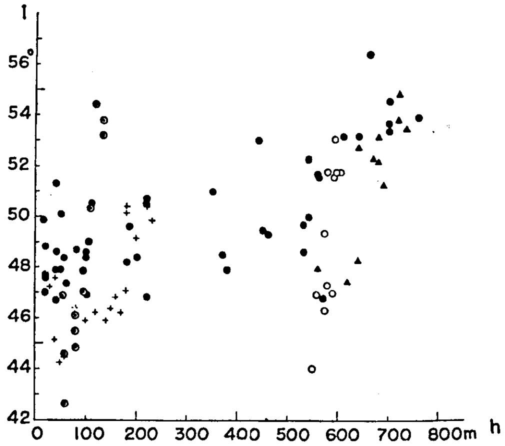

Fig. 2. a) Ooshima Island (Volcano Mihara) after T. Rikitake and I. Yokoyama.

⊙ Mt. Atago.

+ Mt. Takenohira.

○ 604*m* triangulation point on the outer somma.

▲ Mt. Shiraishi on the outer Somma.

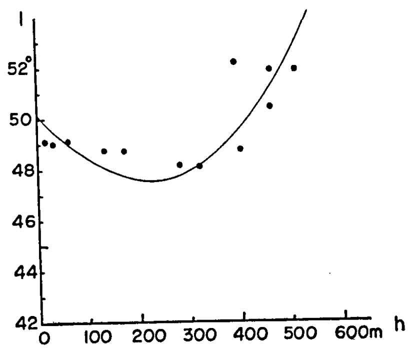

Fig. 2. b) Toshima Island.

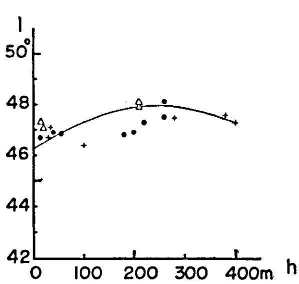

Fig. 2. c) Niizima Island.

● Mt. Mukai-yama.

+ Mt. Miyazuka.

△ Wakagoo.

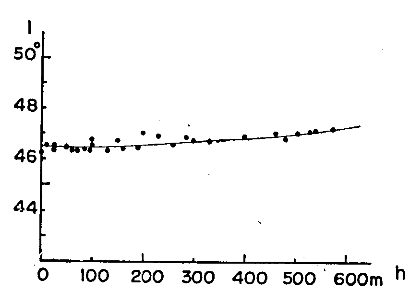

Fig. 2. d) Koozushima Island.

Fig. 2. Dip anomaly and height of the volcanoes in the Seven Izu Islands.

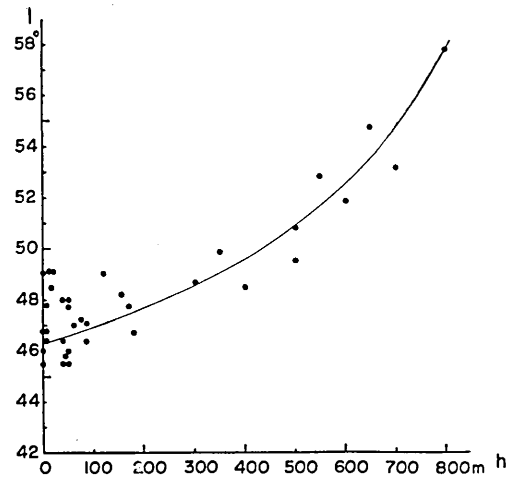

Fig. 2. e) Miyakeshima Island after T. Minakami.

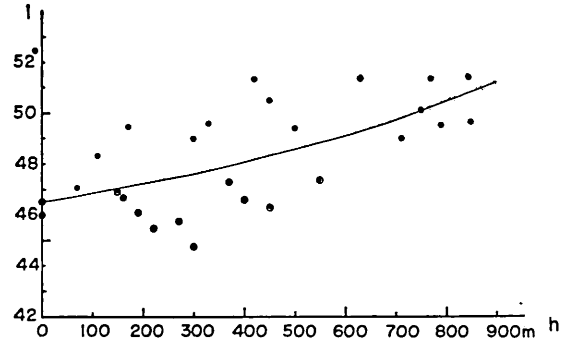

Fig. 2. f) Mikurashima Island.

● on ridge ⊙ in gorge

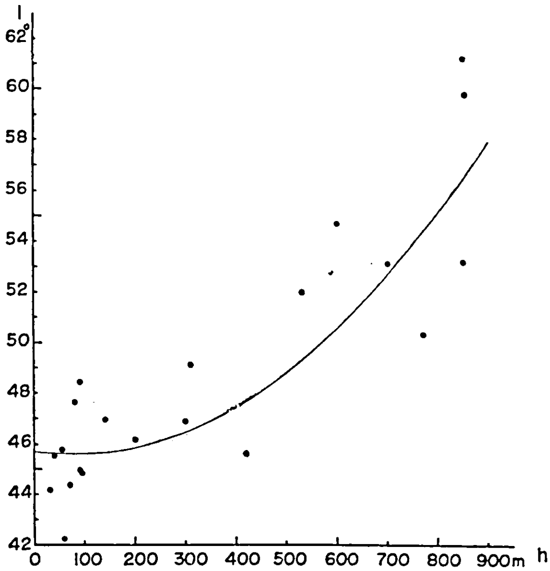

Fig. 2. g) Hachizyo Island (west).

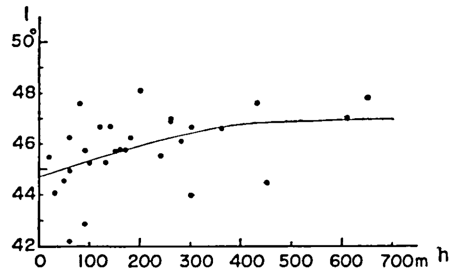

Fig. 2. h) Hachizyo Island (east).

Fig. 2. Dip anomaly and height of the volcanoes in the Seven Izu Islands. (continued)

Table I. Observation of dip on the Seven Izu Islands.

a) Toshima Island.

Time (1954)			Locality		Approximate Altitude	Dip
Aug. 11	12 *h*	30 *m*	No. 1	Village	60 *meters*	49°05′
	13	26	2	N-E slope	130	48 42
		44	3	〃	280	08
	14	07	4	〃	390	52 08
		25	5	〃	460	51 51
		44	6	Triangulation point	508	50 51
	15	16	7	N-W slope	460	20
		36	8	〃	400	48 43
		54	9	〃	320	04
	16	21	10	〃	170	42
	17	18	11	Village	30	49 00
		31	12	Coast	15	04

b) Niizima Island.

Time (1954)			Locality		Approximate Altitude	Dip
Aug. 9	14 *h*	23 *m*	No. 1	Honson Village*	17 *meters*	46°44′
	15	08	101	Mt. Mukai-yama	54	52
		45	102	〃	200	56
	16	04	103	〃	220	47 17
		44	104	〃	260	48 09
	17	20	105	〃	260	47 30
		48	106	〃	180	46 50
	18	22	8	Honson Village*	40	56
10	10	12	107	〃	30	41
		54	108	〃	100	47 24
	11	36	109	Huzimi-pass	280	29
	12	50	110	Mt. Miyazuka	400	20
	13	56	111	〃	380	36
	14	56	112	Shrine	33	06
	15	30	113	Wakagoo Village	15	19
	16	18	114	〃	20	09
		52	115	〃	210	48 04
	17	34	116	〃	210	47 58

* T. Nagata carried out the same observation at these points in 1937. *Bull. Earthq. Res. Inst.*, **15** (1937), 497 (in Japanese).

c) Koozushima Island.

Time (1954)			Locality		Approximate Altitude	Dip
Aug. 6	15 *h*	16 *m*	No. 1	Village	50 *meters*	46°28′
		48	2	Path to Mt. Chichibu	160	22
	16	26	3	Mt. Chichibu	283	52
		58	4	Path to Mt. Chichibu	200	59
	18	22	5	Coast	10	32
7	07	54	6	Path to Mt. Tenzyo-san	85	13
	16	48	7	〃	95	18
	08	52	8	〃	190	27
	09	14	9	〃	260	34
		32	10	〃	330	42
		54	11	〃	400	53
	10	22	12	〃	480	46
	11	22	13	〃	530	47 06
	12	36	14	〃	540	08
	13	12	15	Mt. Kushiga-mine	505	00
	14	24	16	Triangulation point	574	14
	15	22	17	Shiroshima	460	02
		46	18	Path to Mt. Tenzyo-san	300	46 44
	16	19	19	〃	230	18
	17	08	20	〃	70	19
8	08	44	21	Primary School	60	23
	09	04	22	Path to Mt. Chichibu	85	24
		30	23	Middle School	25	20
	12	50	24	Shrine	25	33
	13	38	25	Foot of Mt. Tako	100	33
	14	32	26	Foot of Mt. Nachi	100	40
	15	16	27	Mt. Koodo	230	54
		54	28	〃	150	43
	16	44	29	Nagahama	2	12

d) Mikurashima Island.

Time (1956)			Locality		Approximate Altitude	Dip
Apr. 5	15*h*	54*m*	No. 1	North coast	1 *meter*	46°00′
	16	12	2	〃	1	46 36
	17	10	3	Sato Village	110	48 17
6	07	24	4	Path to Mt. Oyama	160	46 42
		46	5	〃	220	45 28
	08	06	6	〃	300	44 45
		30	7	〃	400	46 36
		56	8	〃	450	46 17
	09	24	9	〃	630	51 18
		46	10	〃	710	48 58
	10	12	11	〃	750	50 06
		48	12	Summit	845	51 24
	12	03	13	Triangulation Point	851	49 35
		25	14	Path to Mt. Oyama	790	49 30
		43	15	〃	770	51 20
	15	35	16	〃	550	47 21
	16	00	17	〃	450	50 28
		24	18	〃	330	49 36
7	07	38	19	Tokkurine-uye	170	49 28
	08	28	20	North east coast	300	49 00
	10	08	21	〃	420	51 19
		57	22	Subarune-uye	500	49 24
	11	40	23	Nango Village	370	47 17
	14	42	24	Kawadagawa	270	45 45
	16	04	25	Usunango	190	46 05
9	14	53	26	Shrine	150	46 56
	15	09	27	Sato Village	70	47 03

e) Hachizyo Island.

Time (1954)			Locality		Approximate Altitude	Dip
Aug. 26	09*h*	28*m*	No. 1	Homei Shrine	60 *meters*	44°58′
	10	07	2	Yokomaga-hara	90	42 53
		48	3	Igona	60	46 16
	11	18	4	Kashidate Village	100	45 17
	12	56	5	〃	160	50
	13	22	6	〃	200	46 06
		46	7	Path to Mt. Higashi-yama	300	44 01
	14	09	8	〃	450	44 27
	15	05	9	Summit of Mt. Higashi-yama	650	47 46
		55	10	Path to Mt. Higashi-yama	610	02
	16	16	11	〃	430	38
		36	12	〃	360	46 34
		54	13	〃	200	48 06
	17	18	14	〃	140	46 42
	18	04	15	Shoobu-soo	50	44 37
27	08	30	16	Meiji High School	80	47 35
	09	15	17	Path to Mt. Nishi-yama	140	46 52
		33	18	〃	200	46 08
		57	19	〃	310	49 03
	10	13	20	〃	420	45 32
	11	06	21	〃	600	54 37
	12	43	22	Summit of Mt. Nishi-yama	850	61 04
	13	30	23	〃	850	53 03
	14	23	24	Triangulation Point	854	59 40
	16	01	25	Path to Mt. Nishi-yama	770	50 14
		23	26	〃	700	53 02
		43	27	〃	530	51 52
	17	26	28	〃	300	46 46
	18	07	29	〃	95	44 46
		23	30	〃	90	48 22
28	11	52	31	Nakanogoo Village	150	45 45
	12	27	32	Road to Sueyoshi Village	240	33
	13	10	33	Sueyoshi Village	180	46 15
	15	08	34	Sueyoshi Prim. School	90	45 48
		53	35	Sueyoshi Village	130	17
29	10	41	36	Ookago Village	60	42 11
	11	06	37	〃	55	45 41
		30	38	〃	70	44 16
		50	39	〃	90	56
	13	09	40	Yaene	20	45 30
	14	33	41	Ookago Village	30	44 06
30	14	08	42	Path to Mt. Higashi-yama	120	46 42
		58	43	〃	280	08
	15	26	44	〃	300	39
		54	45	〃	260	58
	16	35	46	〃	260	54
	17	27	47	Radio Relay Station	170	45 49

anomalies on Volcanoes Asama, Sakurazima and Huzi (Fuji). And the latter approximation was offered by T. Rikitake[7] who tried to interpret the geomagnetic anomalies on Volcano Mihara, Ooshima Island. The effective intensity of magnetization of these volcanoes to cause the observed geomagnetic anomalies, which was obtained by the above methods, is listed in Table II where the mountain-masses are all assumed to be uniformly magnetized.

In these methods, we must assume the uniform magnetization of the mountain-mass, namely the subterranean structure and the effective dimension of the volcano which are, the writer thinks, the final aims for us to achieve in volcanology! And the obtained values of the effective intensity of magnetization as shown in Table II are not comparable, strictly speaking, with those of the rock-specimens near the earth-surface because the subterranean structure of the volcanoes is not always the same as their visible parts and moreover, intensity of rock-magnetization takes rather scattered values as will be discussed in a later part of this paper. Therefore, the writer regards the above-mentioned method as one of the possible second approximations, and

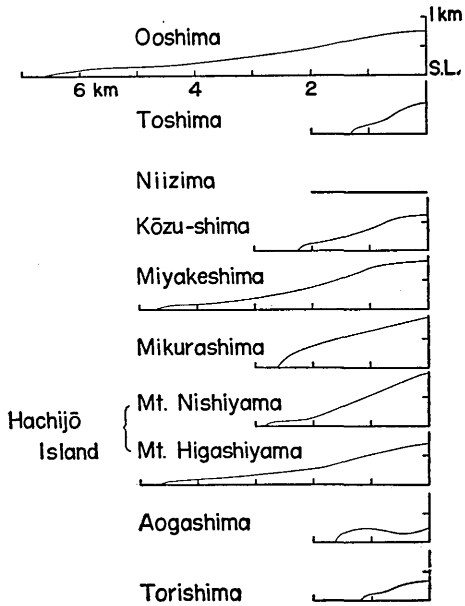

Fig. 3. Topographic profiles of the Seven Izu Islands.

Table II. Effective intensity of magnetization of the volcanoes obtained by various assumptions.

Volcano	Max. Height	Assumption	J *emu/cc*	SiO_2 %	Surveyor
Asama	2532 *m*	One ellipsoid	0.0022	62.1	T. Minakami
Sakurazima	1230	Two ellipsoids	0.0018	62.1	〃
Huzi	3776	Four 〃	0.03	51.4	〃
Ooshima	755	Circular cone	0.037	51.8	T. Rikitake

7) T. RIKITAKE, *loc. cit.* (3).

representation by a dipole-field as the first approximation which contains two factors, moment and depth of the dipole. Approximation by the dipole-field will play a role in determining the subterranean structure of volcanoes together with other methods such as gravimetric, seismometric and geological ones though it remains as the first approximation.

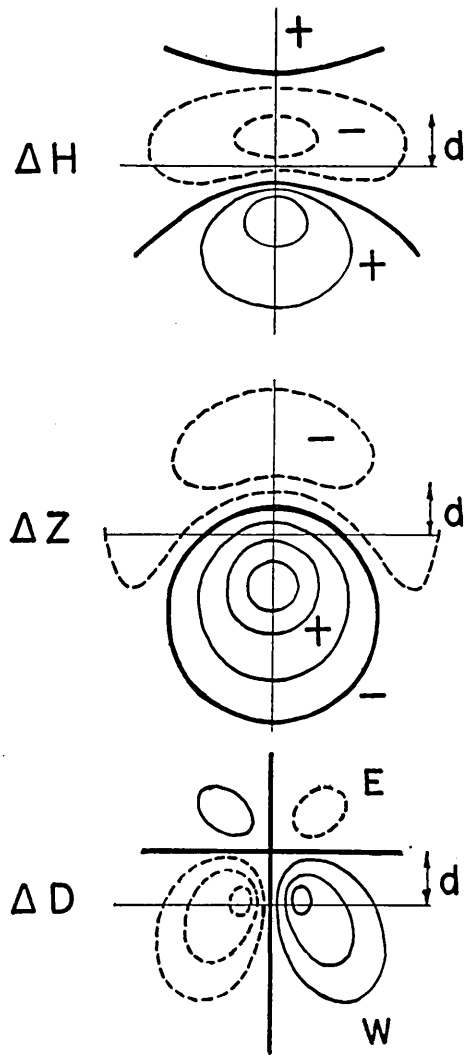

Fig. 4. Distribution of magnetic anomaly due to a underground dipole (d denotes the depth of dipole).

Taking the dipole as the origin of the cordinates and its depth as d, we get the components of geomagnetic anomaly due to the dipole after some elementary calculations,

$$\Delta H = M_z\left[\frac{1}{r^3} - \frac{3x}{r^5}\left(x + d\frac{Z_0}{H_0}\right)\right], \tag{1}$$

$$\Delta Z = 3M_z\left[\frac{-d}{r^5}\left(x - d\frac{Z_0}{H_0}\right)\frac{H_0}{Z_0} - \frac{1}{3r^3}\right], \tag{2}$$

$$\tan \Delta\delta = 3M_z\frac{y}{r^5}\left(\frac{x}{Z_0} - \frac{d}{H_0}\right), \tag{3}$$

where M and $\Delta\delta$ represent moment of the dipole and anomaly in declination respectively. The distribution of anomaly in the central part of Japan where geomagnetic inclination is approximately 45°, namely $H_0 \doteqdot Z_0$, is shown in Fig. 4. And Fig. 5 represents the distribution of three-components of the geomagnetic field observed on Volcano Mihara. In discussing geomagnetic anomaly, to consider the general mode of distribution is more plausible than the observed values at every point. For convenience, the writer, here, pays attention especially to the zero-line in the

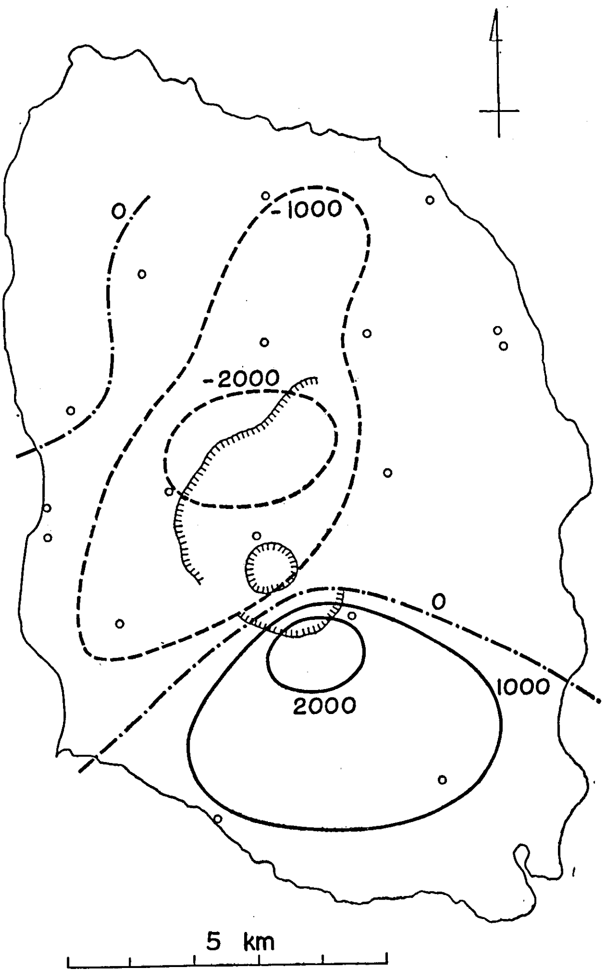

Fig. 5. a) Distribution of anomaly in the horizontal component in *gamma*. Normal field is 30000 *gamma* for 1956.0.

distribution of respective component in Fig. 5. Comparing Fig. 5 with Fig. 4, we can safely obtain the conclusion that the geomagentic anomaly on Volcano Mihara is nicely approximated by the field due to the subterranean dipole, of which the depth is about 2.7 *km*.

If we assume the dipole to be due to a uniformly magnetized sphere, its moment is expressed as follows according to its cause of magnetization whether induction by the earth-field or natural remanent magnetization (N.R.M.),

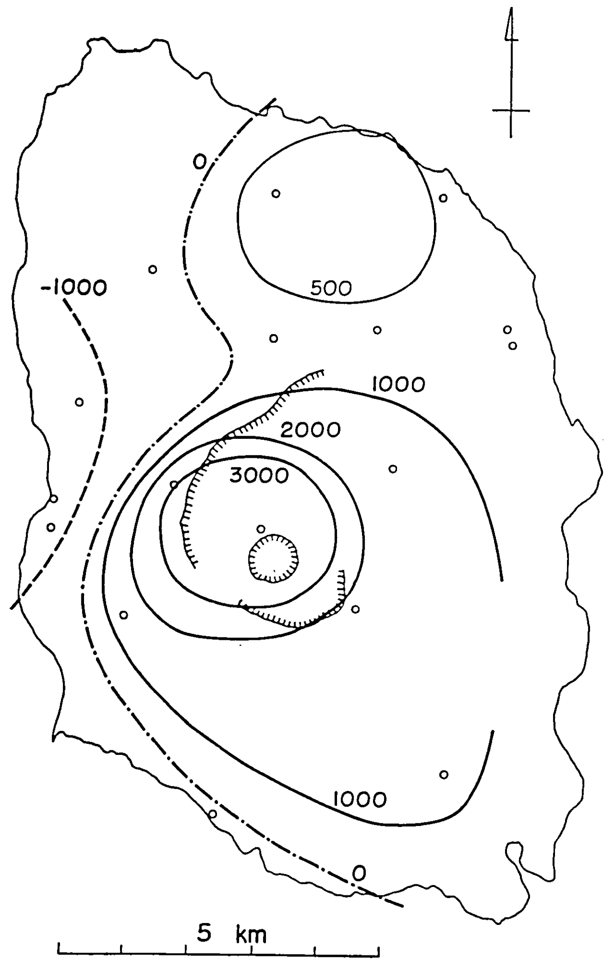

Fig. 5. b) Distribution of anomaly in the vertical component in *gamma*. Normal field is 34000 *gamma* for 1956.0.

$$M=\frac{4/3\cdot\pi R^3\kappa}{1+4/3\cdot\pi\kappa}F_0\,, \tag{4}$$

or

$$M=\frac{4}{3}\pi R^3 J\,, \tag{5}$$

where κ, J, R, and F_0 denote susceptibility, intensity of N.R.M., radius of the sphere and total intensity of the earth-field respectively.

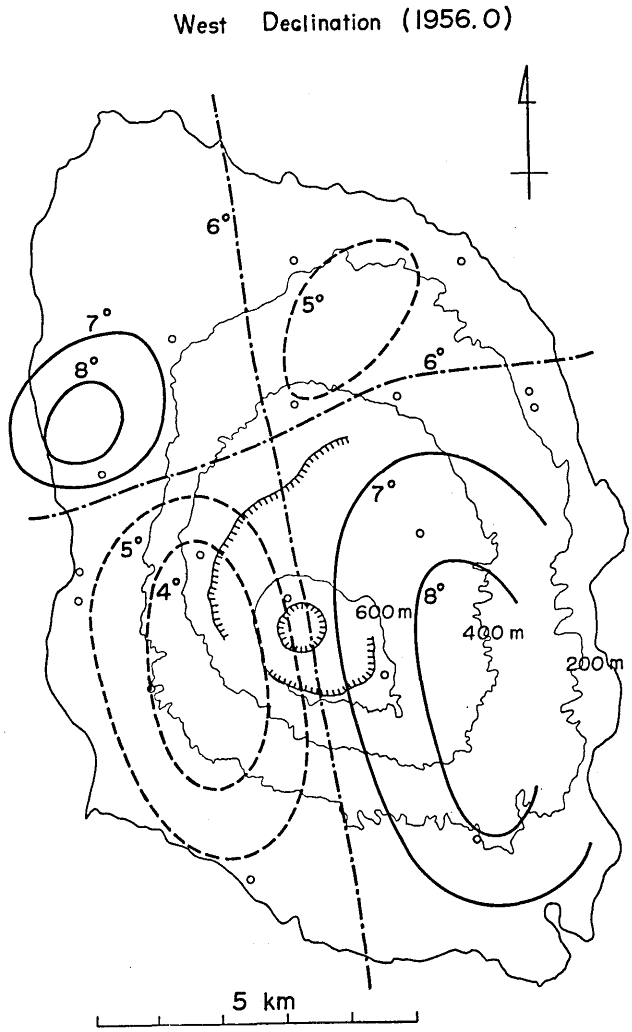

Fig. 5. (c) Distribution of anomaly in the westward declination in *degree*.

Assuming that the dipole is situated beneath the centre of the volcano and H_0 equals Z_0, we consider the following expression relating to dip-anomaly which has been most frequently observed,

$$f(\Delta I)=\frac{\tan(I_0+\Delta I)-\tan I_0}{\tan I_0}=\frac{\Delta Z}{Z_0}-\frac{\Delta H}{H_0}\,. \qquad (6)$$

At the top of the volcano, in other words, right above the dipole,

$$f(\Delta I)=\frac{1}{H_0}\left(2\frac{M_z}{d^3}+\frac{M_x}{d^3}\right)=\frac{3}{d^3}\frac{M_x}{H_0}. \qquad (7)$$

As for Volcano Mihara, $I_0=48°$, $\Delta I=6°$, $H_0=0.32\,emu$ and $d=2.7\,km$, we get

$$M_x(=M_z)=4.9\times10^{16}\,emu\,, \qquad (8)$$

and

$$M=7.1\times10^{16}\,emu\,. \qquad (8')$$

Table III. Magnetization of volcanoes in the Seven Izu Islands.

Volcano	Max. Height	I_0	I_{max}	$f(\Delta I)$	$J(emu/cc)$ $R=d$	$J(emu/cc)$ $R=2d$
Ooshima	755 m	47°45′	54°30′	0.27	9.8×10^{-3}	7.8×10^{-2}
Toshima	508	47 30	52 45	0.20	7.3×10^{-3}	5.8×10^{-2}
Niizima	428	47 20	48 09	0	—	—
Koozushima	574	47 10	47 14	0	—	—
Miyakeshima	814	47 00	57 30	0.46	1.7×10^{-2}	1.4×10^{-1}
Mikurashima	851	46 40	50 45	0.16	5.7×10^{-3}	4.6×10^{-2}
Hachizyo (W)*	854	45 30	56 30	0.48	1.7×10^{-2}	1.4×10^{-1}
Hachizyo (E)*	701	45 30	47 00	0.05	1.8×10^{-3}	1.4×10^{-2}

Volcano	N.R.M. J_n (emu/cc)	κF_0 (emu/cc)	Rock	Recent Activity
Ooshima	$1.2\sim6.7\times10^{-2}$	$0.35\sim2.5\times10^{-3}$	Basalt	1950, 51, 53
Toshima	$3.0\sim6.5\times10^{-2}$		Basalt	?
Niizima	7.8×10^{-4}		Liparite	886
Koozushima	$2.1\sim3.2\times10^{-4}$		Liparite	838
Miyakeshima	$1.2\sim5.6\times10^{-2}$	$0.43\sim1.5\times10^{-3}$	Basalt	1940
Mikurashima	$1.0\sim4.3\times10^{-3}$		Basalt & Andesite	?
Hachizyo (W)*	$1.4\sim32\times10^{-3}$		〃	1605
Hachizyo (E)*	$1.3\sim70\times10^{-3}$		〃	?

* Rock samples were offered by N. Isshiki.

If we assume the shape of the magnetic material corresponding to the dipole to be a sphere, its radius will be obtained as follows according to its effective intensity of magnetization,

$$J=0.01\,emu/cc: \quad R=2.6\,km\,,$$

$$J=0.05\,emu/cc: \quad R=1.5\,km\,.$$

Considering that the depth of the dipole beneath Volcano Mihara is about 2.7 *km*, the above value of the effective intensity of magnetization 0.01 *emu/cc* is very suggestive.

In a general case at the central part of Japan, we get

$$f(\Delta I)=\frac{3}{d^3}\frac{M_x}{H_0} \quad \text{and} \quad M_x=\frac{4}{3}\pi R^3 J\cos 45^\circ\,. \qquad (9)$$

And assuming $d=R$ and $d=2R$, we get the effective intensity of magnetization of the mountain-mass as follows,

$$d=R\ : \quad J=\frac{f(\Delta I)}{4\pi}F_0\,,$$

$$d=2R: \quad J=\frac{2f(\Delta I)}{\pi}F_0\,.$$

Observed and calculated values on the volcanoes in the Seven Izu Islands are listed in Table III. As will be fully discussed in later sections, it may be most natural that the intensity of magnetization of the mountain-mass J is smaller than N.R.M. J_n of rock-specimens near the earth-surface and larger than or equal to κF_0. Thus, we shall learn which of the two assumptions $R=d$ or $R=2d$ is more plausible in our estimation. As for Volcano Mihara, assuming that $R=d$ and both these values are equal to 2.7 *km* as previously obtained, a schematic model will be shown as Fig. 6.

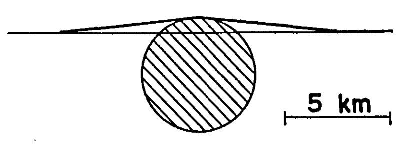

Fig. 6.

Parenthetically the writer may add that the geomagnetic anomalies on the lava-domes or volcanic necks of which the geological structures are known, should be exactly interpreted by the magnetization of the rock-samples and their configurations.

2. Magnetization of igneous rocks and its range

Magnetization of rocks presents different features according to their origin, sedimentary or igneous. Here, we consider the basaltic rocks as an example of the igneous rocks. Order of magnitude of natural remanent magnetization (N.R.M.) and susceptibility of those rocks are

Table IV. Order of magnitude of intensity of N.R.M. and susceptibility of rocks.

Rock	Intensity of N.R.M. $J_n(emu/gr.)$	Susceptibility $\chi(emu/gr.)$	Induced magnetization by earth-field $\chi F_0(emu/gr.)$	$Q=J_n/\chi F_0$
Sedimentary	10^{-6}	10^{-4}	5×10^{-5}	0.02
Igneous	10^{-2}	10^{-3}	5×10^{-4}	20

shown in Table IV where direction of N.R.M. generally coincides with that of the earth-field as studied by T. Nagata[8] and Fig. 7 shows, as an example, the direction of N.R.M. of the rocks from Mikurashima Island while order of their intensities are 10^{-4} *emu/gr*. Various kinds of ejecta from a volcano contribute to the magnetization of the volcano as a whole in different ways. Lava-flows have a large share in forming the N.R.M., while fragmentary ejecta and ashes share mainly in forming the induced magnetization. Therefore, it may be very important in discussing the geomagnetic anomaly on the volcano to assume the composition and distribution of ejecta in the mountain-mass.

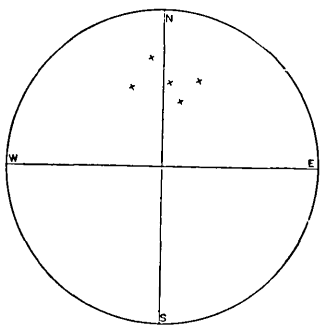

Fig. 7. Schmidt projection of magnetization of rocks from Mikurashima Island (after K. Kobayashi).

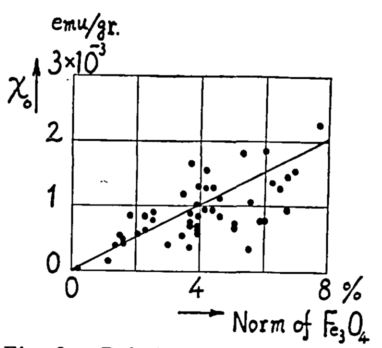

Fig. 8. Relation between specific susceptibility and norm of Fe_3O_4.

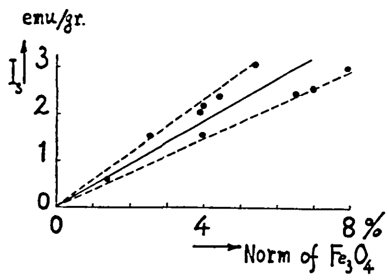

Fig. 9. Relation between saturated magnetization and norm of Fe_3O_4.

8) T. NAGATA, *Bull. Earthq. Res. Inst.*, **19** (1940), 402.

The ranges of distribution of N.R.M. and susceptibility are rather wide as shown in Table III where large values amount to twice or fifty times small ones though numbers of sampling do not always attain a high enough figure. If we assume the uniform magnetization of the mountain-mass, geomagnetic anomaly on the mountain should increase in exact proportion to the assumed intensity of magnetization. In this respect, it seems rather dangerous to attach a very high value to the intensity of magnetization of rocks.

The relation between geomagnetic anomaly on volcanoes and property of rocks composing the volcanoes is easily seen in Table I where basaltic volcanoes present large anomalies and liparitic ones almost none. This may be very natural considering T. Nagata's studies[9] shown in Figs. 8 and 9 which give the relation between magnetic susceptibility and intensity of saturation magnetization and norm of Fe_3O_4 in igneous rocks respectively, while the norm of Fe_3O_4 is inversely proportionate to the silica percentage in general.

As seen from Table IV, the Q-factor of igneous rocks is very large compared with sedimentary ones and a contrast between them equals $10^{-2}/5\times10^{-5}=200$. This value suggests the utility of the magnetic method in studying the subterranean structure of volcanoes which are composed of basaltic rocks. In special cases, the geomagnetic method will be more effective than the gravimetric one contrary to our common sense in potential theory. To take an ideal example, the writer will show the geomagnetic and gravity anomalies due to a buried sphere of which the radius is R. Both anomalies at the place r distant from the centre of the sphere are given as follows.

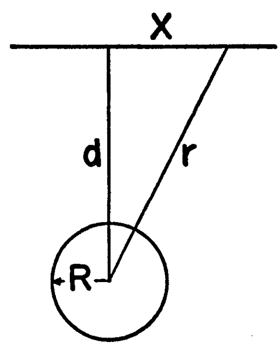

Fig. 10.

$$\Delta g=\frac{4}{3}\pi\cdot R^3k^2\Delta\rho\cdot d/r^3\ , \tag{10}$$

and

$$\Delta Z=\frac{4}{3}\pi\cdot R^3\,\Delta J\left(-x^2+2d^2-3xd\frac{H_0}{Z_0}\right)\,. \tag{11}$$

At the place right above the sphere,

9) T. NAGATA, *Rock-magnetism* (1953), 89 and 106.

$$\Delta g=\frac{4}{3}\pi R^3 k^2\cdot\Delta\rho\cdot 1/d^2\ , \tag{12}$$

and

$$\Delta Z=\frac{4}{3}\pi R^3\cdot 2\cdot\Delta J\cdot 1/d^3\ . \tag{13}$$

It may be safely assumed that both kinds of the contrast $\Delta\rho$ and ΔJ amount respectively 1.0 *cgs* and 0.02 *cgs emu* in a certain volcanic region. Then, the anomalies are estimated for the case where $R=1\,km$ and $d=2\,km$ as

$$\Delta g=14\,mgal \qquad \text{and} \qquad \Delta Z=1000\,\gamma\ .$$

Of these two quantities, geomagnetic anomaly may be more easily detected. In fact, it should be stressed that the abovementioned example is a special case. And here it may be remarked incidentally that geomagnetic anomalies on volcanoes may sometimes change accompanied by their activities as revealed by Japanese geophysicists[10].

3. Bulk-density of the mountain-mass

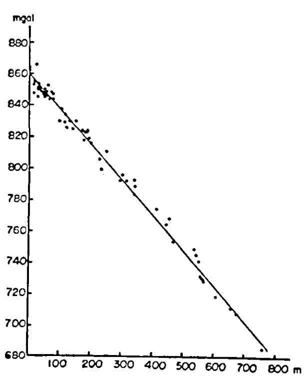

Fig. 11. Relation between observed gravity values and height.

In relation to the subterranean structure of volcanoes, the writer, here, considers the bulk-density of the mountain-mass as a whole regarding a few examples of volcanoes.

a). Volcano Mihara The writer and H. Tajima[11] carried out a gravity-survey on Volcano Mihara by means of a Worden Gravimeter and the relation between observed gravity values and height is shown in Fig. 11. Neglecting the topographical effects and assuming the uniform distribution of density, gravity at the height *h meters* is expressed as

$$g_h=g_0-0.3086\,h+2\pi k^2\rho h\ \ (mgal)\ , \tag{14}$$

10) T. NAGATA, *Bull. Earthq. Res. Inst.*, **19** (1941), 335.
R. TAKAHASI and K. HIRANO, *Bull. Earthq. Res. Inst.*, **19** (1941), 82 and 373.
Y. KATO, *Proc. Imp. Acad. Japan*, **16** (1940), 440.
T. RIKITAKE and I. YOKOYAMA, *Journ. Geophys. Res.*, **60** (1955), 165.

11) I. YOKOYAMA and H. TAJIMA, *Bull. Earthq. Res. Inst.*, **35** (1957), 23.

where ρ is the effective density of the mountain-mass above the sea-level. By the least square method, the density was determined as 2.08 *gr./cc*. This value is rather smaller than that of the ejected lava.

b) Volcano Asama T. Minakami[12] obtained the mean density of Volcano Asama as 1.88 *gr./cc* from the observations of second derivatives of the gravity potential by a torsion balance. And his additional remarks are as follows: Borings made on the eastern slope of the volcano showed that the layers down to 50 *m* under the surface are alternations of pumice, sand, and ash, their mean bulk density being less than 1.3 *gr./cc*, so that in order to arrive at the mean density of the volcano (1.88) obtained above, it was necessary to assume, owing to increasing weight material, that deeper than 50 *m* from the surface, the density would exceed 1.88 *gr./cc*.

In addition the above examples, T. C. Mendenhall[13] and A. Tanakadate swung the pendulums on the summit of Mt. Huzi and obtained 2.08 *gr./cc* as the mean density of the mountain-mass as early as in 1881.

Taking into consideration that the bluk-density of the rocks composing the lava-flows is about 2.5 *gr./cc*, the effective density of the mountain-mass 2.0 *gr./cc* obtained at the above volcanoes may show that volcanoes are composed of various ejecta including lava-flows, pumices, bombs and ashes which are never uniformly magnetized as a whole. Thus the effective density of the mountain-mass bears a close relation to the determination of the effective intensity of magnetization in the assumption of uniform magnetization of the mountain-mass as ellipsoids or a circular cone.

4. Determination of depth of sources by analysing the vertical component in the geomagnetic field on Volcano Mihara

With the aid of E. H. Vestine and N. Davids' method[14] which has already been applied to the analysis of the local anomalous changes of geomagnetic field on Volcano Mihara during the period from 1951 to 1953 by the present author[15], an estimation of the depth of sources responsible for the local anomalous geomagnetic field on the same volcano will be made.

12) T. MINAKAMI, *Bull. Earthq. Res. Inst.*, **20** (1942), 40.
13) T. C. MENDENHALL, *Memo. Sci. Dep.*, (*Tokyo Daigaku*), **5** (1881).
14) E. H. VESTINE and N. DAVIDS, *Terr. Mag.*, **50** (1945), 1.
15) I. YOKOYAMA, *Bull. Earthq. Res. Inst.*, **32** (1954), 169.

The writer assumes the form of the volcano to be a circular cone and takes into consideration the fact that each observation point is not distributed on the same horizontal plane. Denoting the magnetic potential of the local anomalous field by ΔW and using Fourier series and Bessel functions, the solution of Laplace's equation is expressed as

$$\Delta W=\sum_{k=0}^{K}\sum_{n=0}^{N} e^{kz}[A_{kn}\cos n\phi+B_{kn}\sin n\phi]J_n(kr)\,, \qquad (15')$$

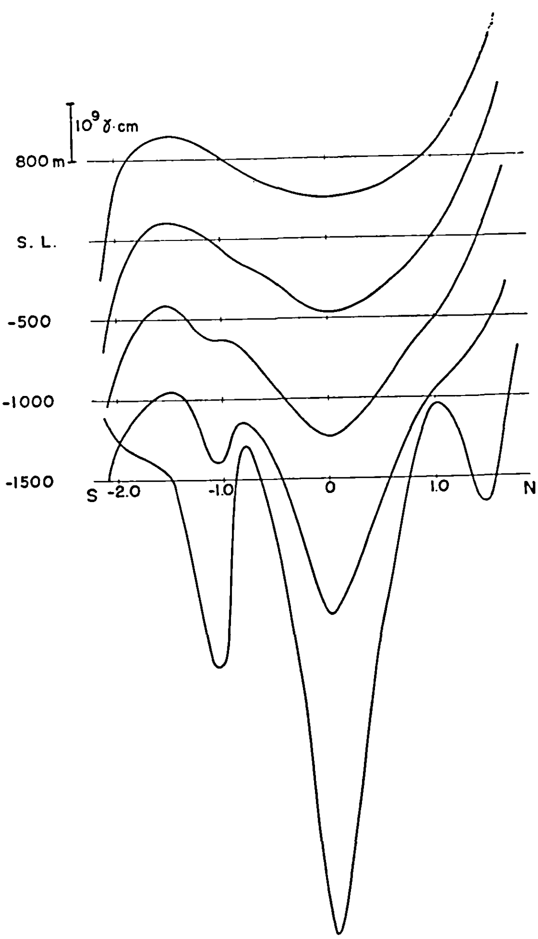

Fig. 12. Distribution of ΔW on the various horizons in the NS direction.

where k and n are positive integers, A_{kn} and B_{kn} are constants and $J_n(kr)$ is a Bessel function of the first kind. For convenience' sake, the distribution of the vertical component ΔZ is considered here. By differentiating (15), ΔZ is obtained as

$$\Delta Z=-\sum\sum ke^{kz}[A_{kn}\cos n\phi + B_{kn}\sin n\phi]J_n(kr)\,. \qquad (16)$$

Then, a set of six concentric circles is drown on Fig. 5 (b), a map of the ΔZ distribution and the Fourier analysis for each circle affords six coefficients.

The constants A_{kn} and B_{kn} in equation (16) are determined by means of the least square method. Using these coefficients, ΔW on the various horizons in the NS direction are calculated by eq. (15) and shown in Fig. 12. As may be seen in the figures, the distribution of ΔW at a depth less than 1 km is fairly convergent, while it seems more divergent as the depth becomes greater. Hence, we may suppose that the sources are to be found at more than 1.5 *km* depth under the sea-level. It may be possible to consider the position of the abovementioned sources as that of the magnetic dipole.

5. Some knowledge obtained by a gravity survey on Volcano Mihara

The results of the gravity survey on Ooshima Island have already been reported in this Bulletin[16]. The Bouguer anomaly is reproduced

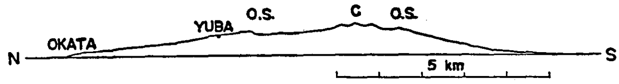

Fig. 14. Topographic profile of Volcano Mihara, Ooshima Island in NS direction.

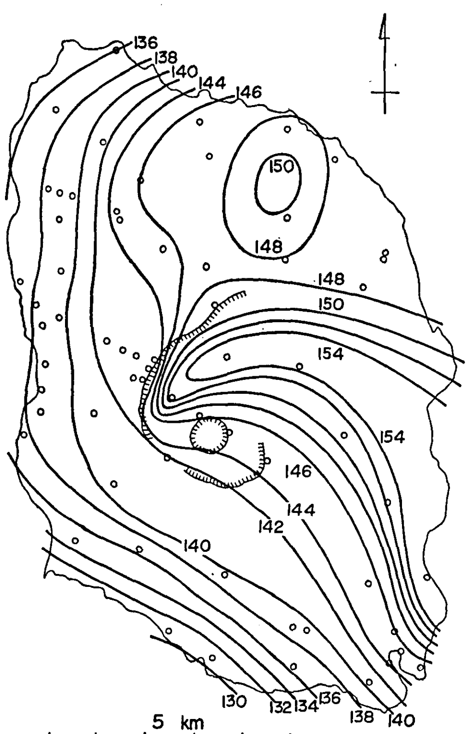

Fig. 13. Distribution of the Bouguer anomaly in *mgal*.

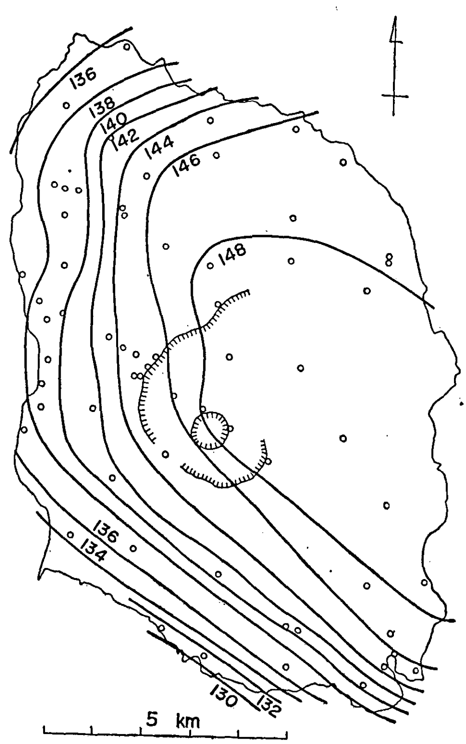

Fig. 15. Distribution of the Bouguer anomaly in *mgal*. (adopting the modified Bouguer corrections).

16) *loc. cit.* (11).

in Fig. 13 which suggests the existence of a subterranean mass of high bulk-density at two parts in the island. One of them, gravity high at the northern part corresponds to the positive anomaly in the geomagnetic vertical component and the anomalous distribution of the horizontal force and declination there. Although we have no visible evidence in geology for the anomaly, the topographical profile of this part covered by the ejecta from Volcano Mihara seems to suggest the existence of an underlying mass which is presumed to be not so large considering the amount of its anomaly. Another high, centered at the central cone and extending the south-east direction, may be taken as indicating the existence of a dense mass of which Hudeshima-Basalts at the eastern

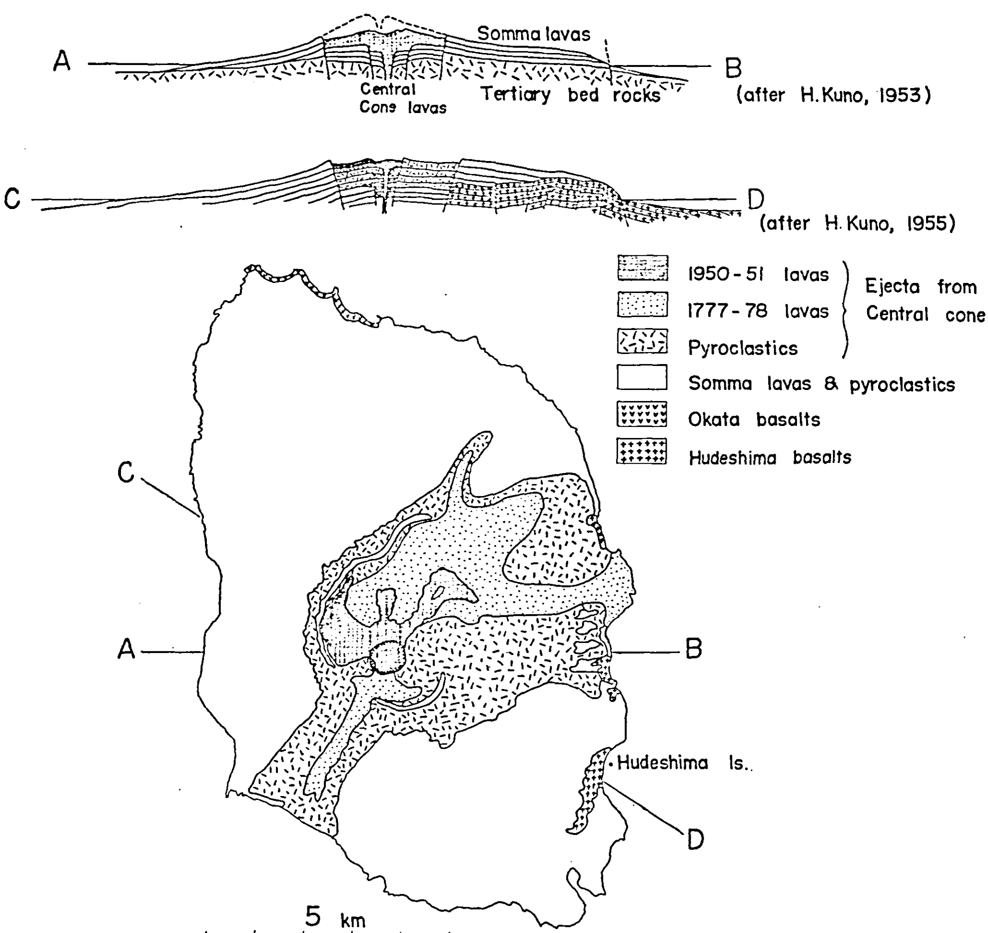

Fig. 16. Geological sketch-map of Ooshima Island after S. Tsuboi and H. Ikuma.

coast of the island may be an outcrop. The fact that the outer somma is in defect in the eastern part of the caldera where the high anomaly prevails, may indicate the existence of dense mass before the caldera subsided. Distribution of the Bouguer anomaly shown in Fig. 9 is obtained by assuming the uniform distribution of bulk-density, that is 2.08 *gr./cc.* As an approximation of higher order, density of rocks at each part of the island was determined by the relation expressed by eq. (14) as discussed in the previous report: 2.40 *gr./cc* for the highly anomalous parts and 2.00 *gr./cc* for the other parts. Using these values of density for the Bouguer correction, the gravity anomaly corresponding to the excess mass under the sea-level was obtained as shown in Fig. 15.

Here, the writer will only refer briefly to the geological perspective over Ooshima Island according to H. Kuno. In 1953 Kuno[17] obtained the geological section as Fig. 16 (AB) and he revised it as shown in Fig. 16 (CD) together with geological sketch map in 1955. As seen from the figures, the result of his studies substantially agrees with that of the gravity survey especially in the subsurface structure. Though we have few geological proofs at the present, geomagnetic and gravimetrical information may afford some clues to the deeper structure of the volcano, in other words, the existence of a rather massive mass beneath the central part of the island similar to the early stage of Volcano Mull[18] in Scotland which has the calderas of Glencoe type of H. Williams as well as Volcano Mihara.

6. Some discussions on parasitic cones of volcanoes

As already shown in Section 2, the distribution of dip-angle on Volcano Mihara is one of the typical examples of geomagnetic anomalies on the basaltic volcanoes. On this volcano, the writer has carried out more minute dip-surveys in succession, especially on the parasitic volcanoes. The results are shown in Table V and also contained in Fig. 2 and discriminated between the four parasitic cones and other slopes in Fig. 20. Fig. 2 shows the general tendencies of geomagnetic anomaly of the whole volcano excepting the parasitic cones. Interpreting the distribution of dip anomaly shown in Fig. 20 as geomagnetic profiles in

17) H. KUNO, *Trans. Amer. Geophys. Union,* **34** (1953), 276.

18) J. E. RICHEY, *British Regional Geology, Scotland: The Tertiary Volcanic Districts* (1948), 57 (Fig. 26).

exploration, anomaly due to a parasitic cone does not superpose itself on that due to the other parts of the mountain-mass and the general tendency of anomaly all over the volcano seems to be composed of the above respective anomalies.

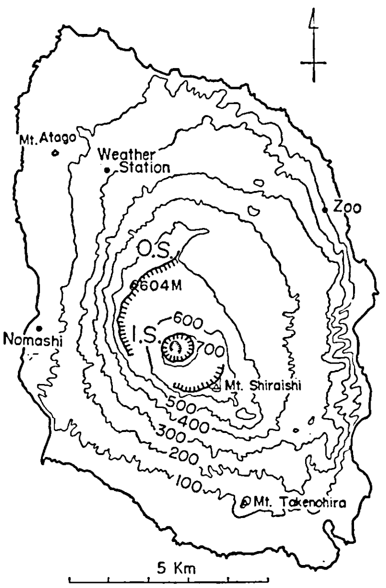

Fig. 19. Topographical map of Ooshima Island.
I.S.: Inner somma.
O.S.: Outer somma.

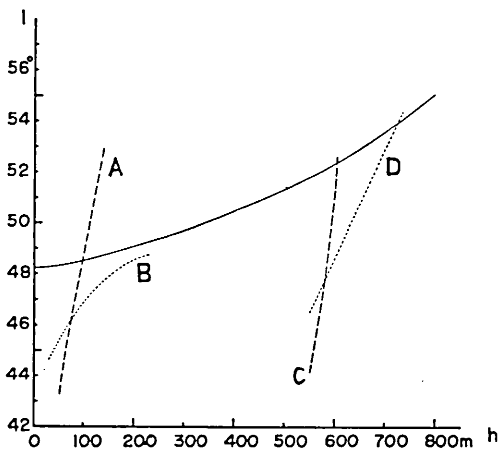

Fig. 20. Dip anomaly on Ooshima Island
A: Parasitic cone Mt. Atago.
B: Parasitic cone Mt. Takenohira.
C: 604 m triangulation point on the outer somma.
D: Mt. Shiraishi on the outer somma.

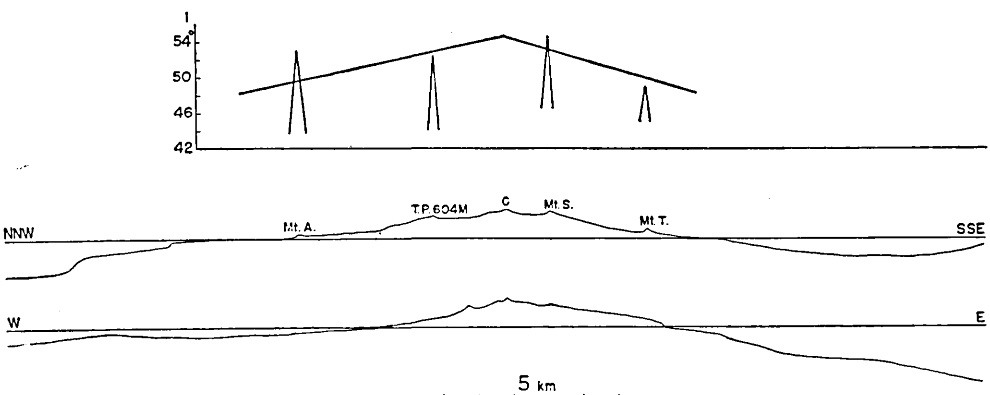

Fig. 21. Geomagnetic profile (dip-angle) and the corresponding topographic profile (NNW-SSE) of Ooshima Island.
A: Atago, T: Takenohira, S: Shiraishi, C: Central cone.

Table V. Observations of dip on the parasitic cones and the outer somma of Volcano Mihara.

a) Mt. Atago.

Time (1955)			Locality		Approximate Altitude	Dip
Apr. 12	15 *h*	49 *m*	No. 1	Southern foot	60 *meters*	44°35′
		57	2	Southern slope	70	46 06
	16	05	3	〃	80	44 51
		13	4	〃	95	47 50
		29	5	Triangulation point		53 12
					135	
		39	6	Summit	135	53 48
		45	7	Western slope	120	54 26
		52	8	〃	105	48 58
	17	01	9	〃	110	50 20
		08	10	Shrine		47 02
					95	
		15	11	Western slope	80	45 30
		23	12	Western foot	60	42 39
		33	13	Cross roads	55	46 54

b) Mt. Takenohira.

Time (1955)			Locality		Approximate Altitude	Dip
Apr. 12	09 *h*	35 *m*	No. 1	Sashikizi Prim. School	30 *meters*	47°14′
		49	2	Shrine	40	47 33
	10	01	3	Southern foot of the hill	60	44 30
		13	4	Southern slope	80	46 23
		26	5	〃	100	45 52
		39	6	Western slope	120	46 13
		53	7	Southern slope	150	46 20
	11	01	8	〃	160	47 02
		11	9	Western slope	200	49 08
		30	10	〃	220	50 26
		39	11	Triangulation point	231	49 51
		55	12	Southern slope	180	50 09
	12	06	13	〃	160	46 48
		14	14	〃	180	50 24
		21	15	〃	170	46 11
		31	16	〃	140	45 56
		48	17	Western foot of the hill	50	44 16
	13	10	18	〃	40	45 09

c) 604 *meters* triangulation point on the outer somma.

Time (1955)			Locality		Approximate Altitude	Dip
Apr. 14	13*h*	05*m*	No. 1	Triangulation point	604 *meters*	51°46′
		20	2	Path to Yuba	595	53 04
		28	3	〃	580	51 48
		54	4	Path to Gojinka-chaya	595	51 36
	14	04	5	〃	580	47 19
		40	6	Inner slope of outer somma	550	43 59
		50	7	〃	560	46 56
	15	03	8	〃	575	46 20
		18	9	〃	590	47 00
		48	10	〃	600	51 46
	16	09	11	Road to Yuba	575	49 24

d) Mt. Shiraishi on the outer somma.

Time (1955)			Locality		Approximate Altitude	Dip
Sept. 16	11*h*	12*m*	No. 1	Western foot	560 *meters*	48°01′
		26	2	Slope of the outer somma	640	48 17
		38	3	Summit of the outer somma	680	53 12
		50	4	〃	690	51 16
	12	39	5	〃	720	53 54
		54	6	Triangulation point	734	53 28
	13	12	7	Eastern slope	720	54 56
		24	8	〃	680	52 10
		34	9	〃	670	52 20
1951 Mar. 30	13	18	30	Eastern slope	640	52 48
1953 Aug. 2	17	44	42	Southern foot	620	47 30

Taking into consideration that the harmonic components of the lower orders of geomagnetic anomaly expressed in the Fourier series are generally due to the deeper origin, the geomagnetic anomaly of the general tendency of the whole volcano shown in Fig. 2 is attributable to the deeper part of the volcano and the anomaly on a parasitic cone is to be interpreted by its own magnetization or rather shallow sources.

Here, the writer will consider the effective bulk-density of the parasitic cones of Volcano Mihara by the same method as used in Section 3. Assuming the vertical gradient of gravity to be constantly 0.3086 *mgal/m*, the relation between the gravity values and the heights is given by

$$g_h = g_0 - 0.3086\, h + 2\pi k^2 \rho h - \delta_t \,, \qquad (17)$$

where ρ and δ_t denote the effective density of the mountain-mass and topographical correction respectively.

On the two parasitic cones of Volcano Mihara, Mts. Atago and Takenohira, the writer observed the gravity values which are shown in Table VI. By eq. (17), the effective density are determined as 0.79 and

Table VI. Gravity values on the parasitic cones of Volcano Mihara.

		Height (*m*)	Observed Gravity (*mgal*)	Topographical Correction (*mgal*)	Bouguer Anomaly (*mgal*)
Mt. Atago	No. 12 Eastern foot	65.1	847.0	3.4	138.8
	〃 13 Top	119.5	829.4	4.7	134.5
	〃 14 Western foot	38.7	852.6	3.5	138.5
Mt. Takenohira	No. 28 Eastern foot	128.0	826.6	3.7	139.3
	〃 29 Top	231.9	796.2	3.5	131.7

0.35 *gr./cc* respectively. Though these values may contain some errors due to the above assumption, the parasitic cones are composed of rather coarse material whether this is the cause or effect of eruptions. This is the same as the region around the central cone of the volcano as mentioned in Section 5.

Next, we consider the topographical effect on geomagnetic anomaly by examples of Volcano Mihara as a whole and a parasitic cone Mt. Atago. According to T. Rikitake[19], dip-anomaly depends on intensity of magnetization J and a topographical constant G as shown by following relation,

19) T. RIKITAKE, *loc. cit.* (3).

$$f(\Delta I)=\{\tan(I_0+\Delta I)-\tan I_0\}/\tan I_0=\Delta Z/Z_0-\Delta H/H_0$$
$$=\pi JG(2\sin\theta/Z_0+\cos\theta/H_0)\ , \qquad (18)$$

where I_0 and θ denote respectively the normal value of dip and the inclination of direction of magnetization. If we fix our eyes on the centre of the top plane of a uniformly magnetized circular cone, G is given by Rikitake as follows.

$$G=\frac{m}{(m^3+1)^{3/2}}\log\frac{\alpha+m^2+1+\sqrt{m^2+1}\sqrt{(1+\alpha)^2+m^2}}{\alpha+\sqrt{m^2+1}\,\alpha}$$
$$+\frac{m}{m^2+1}\left\{\frac{m^2-1-\alpha}{\sqrt{(1+\alpha)^2+m^2}}+1\right\}\ , \qquad (19)$$

where

$$m=\tan\lambda\ , \qquad \alpha=c_0m/h\ ,$$

and where λ, c_0 and h denote the slope of the cone, the radius of the top plane and the height of the circular cone. Using this relation, the effective value of J is obtained by knowing dip-anomaly on the top of the mountain and the topographical constant G.

Volcano Mihara as a whole:

$$I_0=\theta=48^\circ\ ,\quad \Delta I=6^\circ\ ,\quad \lambda=9^\circ\ ,\quad c_0=500\,m\ ,\quad h=700\,m \text{ and } G=0.35$$

Thus we get $J=0.033\,emu/cc$.

Mt. Atago :

$$I_0=\theta=48^\circ\ ,\quad \Delta I=5^\circ\ ,\quad \lambda=25^\circ\ ,\quad c_0=15\,m\ ,\quad h=86\,m \text{ and } G=1.16$$

Thus we get $J=0.008\,emu/cc$. As for Mt. Takenohira, the conditions are almost the same to Mt. Atago. From the above results, we may deduce that the geomagnetic anomaly on the steep mountain is interpreted even by the weak magnetization while the anomaly on the gently-sloping mountain requires the strong and uniform magnetization due to the N.R.M. which is rather unplausible as fully discussed in Section 1. In fact, the magnetizations of rock-samples from Mt. Atago and Mt. Takenohira are obtained as 1×10^{-3} and $3\times10^{-3}\,emu/gr.$ respectively. Namely, the geomagnetic anomaly on Mt. Atago may be due to the magnetization of the mountain-mass mainly by induction. This agrees with the fact that the effective bulk-density of the parasitic cones proved rather small.

7. Geomagnetic anomaly around the craters of volcanoes

T. Fukutomi[20] observed the anomalous distribution of the geomagnetic declination around the crater of Volcano Asama. And T. Nagata[21] observed a similar phenomenon around the crater of Volcano Mihara and concluded that the anomaly can be interpreted as magnetic anomaly, largely due to the uniform magnetization of the central cone with its intensity of 0.0058 *emu/cc* in the direction of geomagnetic force. This magnetization is too large if the rock composing the central cone has solely induced magnetization by the present geomagnetic field, while this is too small if the rock has the natural remanent magnetization observed as $1.6\times10^{-2}\sim3.6\times10^{-2}$ *emu/cc*. Thus he concluded that the central cone of Volcano Mihara is formed not only of continuous ropy lava, but also of bombs, lapilli, ashes and other pyroclastic materials, so that by assuming that lava sheet 6 or 7 *m* thick with natural remanent magnetization $J_n = 0.025$ *emu/gr*. and specific susceptibility $\chi = 6.5\times10^{-4}$ *emu/cc* covers the body of the central cone, composed of pyroclastic ejecta, the magnetic susceptibility of which is almost the same as that of lava, but without any remanent magnetization in the sense of average character of the whole body.

Similarly Nagata presumed that the central cone of Volcano Asama is composed of 40% lava with a magnetization of $\rho(J_n+\chi F_0)$ and 60% pyroclastic ejecta with only induced magnetization $\rho\chi F_0$ where J_n and χ were assumed to be the mean of their observed values. The abovementioned discussions show that the mountain mass of the volcanoes is not always magnetized uniformly simply by N.R.M.

T. Nagata[22] made the geomagnetic measurements and torsion balance survey at eight stations on Ooshima Island in 1938 concerning the magnetization of the subterranean rocks. Assuming that the observed geomagnetic anomaly is due to uniform magnetization of the excess mass that is the cause of the observed anomaly in the second derivatives of the gravity field, he concluded that the subterranean rocks under the earth's surface of Ooshima Island ought to have fairly intense remanent magnetization which is equal to about 0.05 *emu/cc*.

20) T. FUKUTOMI, *Zisin*, **2** (1930), 641.
21) T. NAGATA, *Bull. Earthq. Res. Inst.*, **16** (1938), 288.
22) T. NAGATA. *Bull. Earthq. Res. Inst.*, **17** (1939), 93.

8. Some information obtained by the aeromagnetic surveys over the volcanoes in Alaska

It is very desirable to measure the geomagnetic field at a certain altitude from the earth's surface in order to lessen the topographical effects. In U.S.A. total-intensity aeromagnetic surveys have been carried out at several districts where volcanoes are found. The results in those surveys give some information concerning the subterranean structure of volcanoes, though each volcano may have its own structure. The profile over Mt. Adagdak in the aeromagnetic survey of Adak, Alaska by F. Keller, J. L. Meuschke and L. R. Alldredge[23] is reproduced in Fig. 24, where the computed values of the magnetic field by using the topographic profile and a susceptibility contrast of 0.005 *emu/cc*, are indicated by the small circles plotted with the profiles. The computation gives an approximate fit with the observed profile while the value of 0.005 *emu/cc* is a rather large figure for the susceptibility of a basaltic mass with reference to T. Nagata[24]'s study.

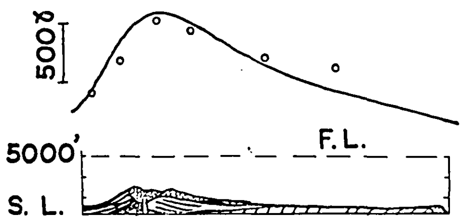

Fig. 24. Magnetic anomaly on Mt. Adagdak, Aleutian. F.L. denotes the fleight level (after F. Keller, J.L. Meuschke and L.R. Alldrege.)

An aeromagnetic map of part of northeastern Umnak, Alaska obtained by the abovementioned authors is also reproduced in Fig. 25 where the flight level is 2000 *m* above sea level. As seen in the

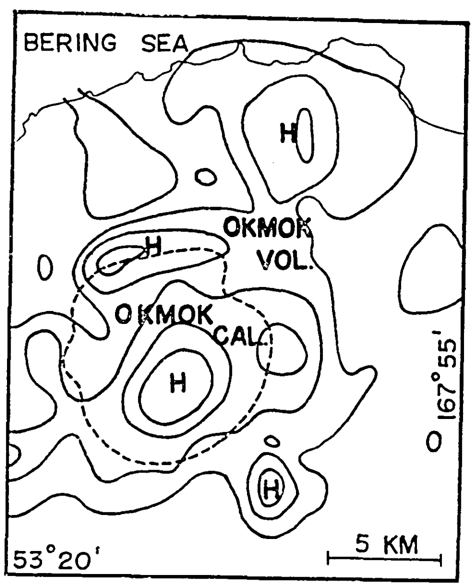

Fig. 25. Aeromagnetic map of part of northeastern Umnak, Alaska. Contour-line interval is 250γ (after F. Keller, J.L. Meuschke and L.R. Alldrege.)

23) F. KELLER, J. L. MEUSCHKE and L. R. ALLDREDGE, *Trans. Amer. Geophys. Union*, **35** (1954), 558.

24) T. NAGATA, *loc. cit.* (9), 101.

Fig. 17. Aerial view of Ooshima Island from south. Photo. Asahi

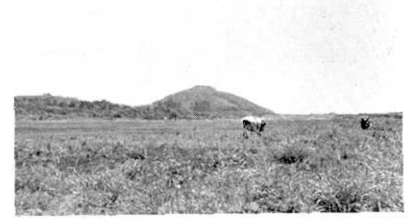

Fig. 22. Parasitic cone Mt. Atago.

Fig. 23. Parasitic cone Mt. Takenohira.

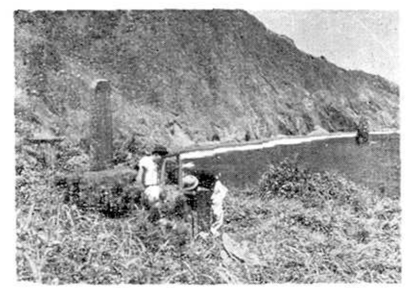

Fig. 18. Gravity survey near Hudeshima Island.

figure, the caldera rim is outlined approximately by the pattern of magnetic contours. There is no magnetic evidence, however, of any of the nine cones, but there is a large anomaly associated with the central part of the caldera. The writer is inclined to think that this is caused by a contrast of magnetization (N.R.M.) rather than by that of susceptibility of the underlying rocks because the latter contrast is not so large.

By these two examples of the aeromagnetic survey it may be said that geomagnetic anomaly related to the topographic configuration of the volcano on a large scale is due to a susceptibility contrast, and a large anomaly deviated from the profile is due to a magnetization (N.R.M.) contrast of the underlying rocks. But geomagnetic anomaly on the massive rocks which were essentially lava-flows such as lava-domes or volcanic necks is attributable to N.R.M. and associated with its topography.

Conclusion

In this paper the writer tried to figure the subterranean structure of the volcano, as an example, Volcano Mihara mainly by means of the geomagnetic methods and discussed the related phenomena to get positive proofs of the structure. As for Volcano Mihara, in fact, we have many problems to solve and many phenomena to observe in addition to the items discussed in this report but the writer made bold to figure some of the plausible subterranean structure of the volcano presumed by the existing data. Though the geomagnetic method by itself may be regarded as approximate, it will give some clues for interpreting the structure of volcanoes together with the gravimetric, seismometric and geological methods.

In concluding, the writer wishes to express his hearty thanks to Dr. T. Rikitake who advised him throughout the course of this study. His sincere thanks are also due to Prof. T. Nagata and Prof. T. Minakami whose valuable work he often referred to in this paper.

---

17. 火山地域における地磁気異常と地下構造

地震研究所 横 山 泉

日本の諸火山の帯磁に関する調査は枚挙に遑がない程，広く行われてきた．そしてこれに対する解釈も 2, 3 出されている．今や，この方法の火山学における有用性を吟味反省すべき時であると考え，若干の考察を試みた．如何なる方法と雖も，単独ではその効力を充分に発揮できないことは勿論である．地磁気異常の研究も他の方法と関連参照することにより，充分有効であると結論する．